

Stopping Power and Collective Flow of Nuclear Matter in the Reaction Ar + Pb at 0.8 GeV/u

R. E. Renfordt and D. Schall

Institute für Hochenergiephysik der Universität, D-6900 Heidelberg, Federal Republic of Germany

and

R. Bock, R. Brockmann, J. W. Harris, A. Sandoval, R. Stock, and H. Ströbele

Gesellschaft für Schwerionenforschung, D-6100 Darmstadt, Federal Republic of Germany

and

D. Bangert and W. Rauch

Fachbereich Physik der Universität, D-3500 Marburg, Federal Republic of Germany

and

G. Odyniec, H. G. Pugh, and L. S. Schroeder

Lawrence Berkeley Laboratory, University of California, Berkeley, California 94720

(Received 29 May 1984)

Charged-particle exclusive data for Ar+Pb collisions at 0.772 GeV/u are analyzed in terms of collective variables for the event shapes in momentum space. Semicentral collisions lead to sideways flow whereas nearly head-on collisions have spherical shapes in the c.m. frame, resulting from complete stopping of projectile motion. The hydrodynamical model predictions agree qualitatively with the data whereas the standard cascade model disagrees, lacking in stopping power and collective flow.

PACS numbers: 25.70.Np

Only in nucleus-nucleus collisions can extended regions of nuclear matter with high energy densities be produced under laboratory conditions. The extent to which nuclear matter can be compressed depends primarily upon the bulk properties of nuclear matter. These determine the degree of thermalization, and the energy density reached in the fireball.¹ An important property which will be addressed in this Letter is the ability of nuclear matter to degrade the initial longitudinal momentum in a nuclear collision, namely the nuclear stopping power. During the interpenetration phase, two mechanisms can reduce the initial longitudinal motion. *Microscopic* baryon-baryon interactions generate random thermal motion and pionic or resonance mass. *Collective* degrees of freedom cause energy to be expended in compression of nuclear matter resulting in a collective flow of energy along the direction of the pressure field gradient.² The two principal dynamic models based on each of these mechanisms provide a complementary set of predictions. The microscopic approach of the intranuclear cascade^{3,4} predicts a forward-backward oriented prolate distribution of nucleon momenta in the fireball center of mass. The hydrodynamic model, on the other hand, presupposes complete nuclear stopping and predicts a prolate sideways

deflection of the incident momentum flux for finite impact parameters and an oblate pattern perpendicular to the beam axis in the zero impact parameter limit.^{5,6}

Several attempts have been made to identify hydrodynamic sideways flow from inclusive⁷ or high-multiplicity-selected inclusive⁸ data with only marginal success. Recently, a sideways deflection of matter was reported⁹ for charged-particle exclusive data in the symmetric Nb+Nb system at 400 MeV/u. To search for collective effects and their influence on the flow of nuclear matter in central collisions of nonsymmetric target-projectile systems, a charged-particle exclusive experiment was carried out for the reaction ⁴⁰Ar+Pb at 0.772 GeV/u. In this Letter results of the event-by-event analysis of a sample of 1000 central-collision events in terms of multiparticle observables are presented. We employ the angle of maximum momentum flow⁶ and the ratio R of the mean transverse momentum $\langle |p_t| \rangle$ to the mean longitudinal momentum $\langle |p_l| \rangle$. The flow angle is sensitive to sideways flow patterns¹⁰ whereas the R ratio measures the degree of stopping and approach to an isotropic distribution.¹¹ As a result of studying these observables it will be shown that near head-on collisions lead to stopping and isotropy whereas side-

wards deflection of flow occurs at intermediate impact parameters.

The experiment was carried out at the Bevalac Streamer Chamber facility. The techniques used in the experiment and data analysis along with a subsample of the present data are published elsewhere.¹¹ The streamer chamber was triggered by requiring that no significant fraction of the projectile nucleus survived the collision. These near-central collisions of Ar+Pb correspond to a trigger cross section of 1.0 b which in a geometrical picture corresponds to a cutoff in the impact parameter at $b \leq 5.5$ fm. A more refined cut in impact parameter was obtained event by event from the multiplicity of participant protons, M_p . The participants were defined as those baryons with momentum per nucleon greater than 270 MeV/c in both the target and projectile c.m. systems. Throughout the subsequent analysis only the energy and momentum carried by the proton in deuterons and tritons were included, thus disregarding not only the unobserved neutrons but also those bound in clusters. The data were compared to the proton distributions of the cascade model of Cugnon *et al.*³ after subjecting the cascade-generated events to a Monte Carlo filtering procedure simulating the experimental biases.

The multiplicity distributions for the participant protons in the data and in the cascade event samples were found to agree well. Furthermore multiplicity subsamples were defined for $M_p > \langle M_p \rangle$ and $M_p < \langle M_p \rangle$, respectively, with $\langle M_p \rangle = 36$. By use of the relationship between b and M_p provided by the cascade model, the samples correspond to near head-on impact parameters $b < 3$ fm, and to intermediate impact parameters $3 \leq b \leq 5.5$ fm, respectively. The analysis in terms of multiparticle variables was restricted to the forward hemisphere of the participant center-of-mass frame in order to circumvent uncertainties resulting from target absorption. The center-of-mass velocity for each event was computed from the momenta of all protons with $p_t > 270$ MeV/c.

Information on the degree of thermalization and nuclear stopping can be obtained on an event-by-event basis from the multiparticle observable¹¹

$$R = \frac{2}{\pi} \frac{\sum_{\nu} |p_{t\nu}|}{\sum_{\nu} |p_{l\nu}|}, \quad (1)$$

which for an isotropic distribution is unity. The p_{ν} are the transverse and longitudinal momentum components of the protons emerging in the forward direction in the participant c.m. frame. Deviations from unity indicate either a preponderance of momentum flow in the direction perpendicular to

the beam ($R > 1$), or partial transparency ($R < 1$). Figure 1 shows event frequencies as contours in the R vs M_p plane where the impact parameter decreases as M_p increases. Approaching from forward oriented shapes ($R < 1$) the dashed curve, which indicates the ridge of the distribution, intersects the isotropy line ($R = 1$) at $M_p = 40$ where complete stopping occurs. In fact, $R = 1$ is only a necessary condition for isotropy. It will be shown below that the momentum flux of events with $M_p = 40$ is indeed spherical. In a clean-cut fireball geometry the mean impact parameter corresponding to $M_p = 40$ is ~ 2.5 fm. Since $r(\text{Ar}) \simeq 4$ fm and $r(\text{Pb}) \simeq 7$ fm the projectile dives completely into the target at this impact parameter. Complete diving thus leads to complete stopping for Ar+Pb at this incident energy. At $M_p > 40$, R exceeds unity indicating a slight excess of transverse over longitudinal momentum components in these events.

The dotted line in Fig. 1 represents the ridge of the corresponding contour plot for cascade events. It does not reach isotropy even for maximum multiplicity; thus the cascade mechanism lacks a significant fraction of the stopping power of the nuclear medium. With $M_p = 40$ the cascade yields $\langle R_{\text{cascade}} \rangle = 0.83$, indicating an excess of longitudinal over transverse energy of approximately 30% in the center of mass. The difference between the observed $R = 1$ and the predicted $\langle R_{\text{cascade}} \rangle$ may be attributed to the generation of compressional (potential) energy, contributing to the stopping power. The compressional energy, not included in the standard cascade model, has recently been estimated¹² to amount to approximately one-third of the

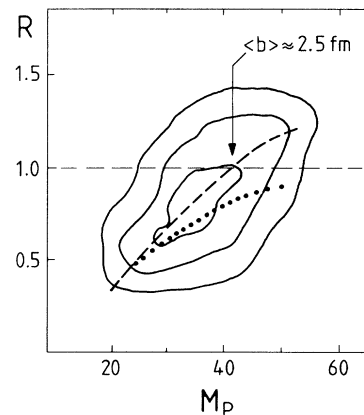


FIG. 1. Contour lines of event frequency in the variables anisotropy coefficient R vs participant proton multiplicity, for the reaction Ar+Pb at 0.772 GeV/u. Dashed (dotted) lines give the ridge of the distributions for the data (the cascade model prediction).

total energy available in the center of mass.

In order to study in more detail the momentum flux pattern the normalized flux tensor⁴

$$T_{ij} = \left[\sum_{\nu} p_{\nu i} p_{\nu j} / |p_{\nu}| \right] \left[\sum_{\nu} |p_{\nu}| \right]^{-1}, \quad (2)$$

$$i, j = x, y, z,$$

is used where $p_{\nu i}$ and $p_{\nu j}$ are the Cartesian components of the c.m. momentum of particle ν and p_{ν} the total c.m. momentum. The event shape in momentum space is defined by the normalized eigenvalues and eigenvectors of T_{ij} . Only protons in the forward hemisphere of the c.m. are included (as in the R ratios discussed above). From among the five independent parameters describing T_{ij} the "flow angle" θ between the direction of the main tensor axis and the beam will be emphasized. Figure 2(a) gives the flow angle distribution $dN/d \cos \theta$ as a function of θ for the multiplicity samples corresponding to impact parameters $b < 3$ fm and $3 \leq b \leq 5.5$ fm, respectively. The high-multiplicity (small impact parameter) events exhibit a fairly flat angular distribution, indicative of a nearly isotropic momentum flow with a slight suppression at forward angles.⁸ Events with $3 \leq b \leq 5.5$ fm exhibit a definite sideways deflection of flow angles away from the beam axis. This deflection is predicted by

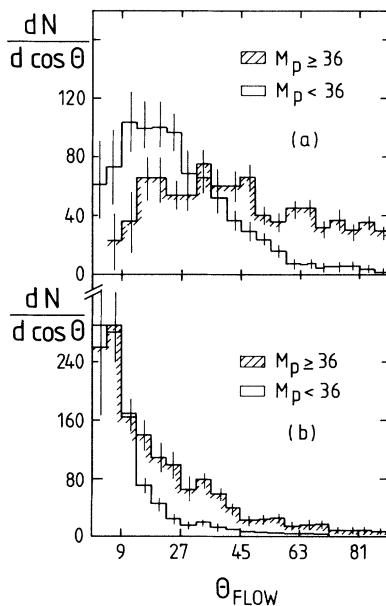


FIG. 2. (a) Distributions of the angle of maximum momentum flow in the c.m. frame for Ar+Pb events with participant proton multiplicities smaller and larger than $\langle M_p \rangle$. (b) Same for the corresponding samples of cascade model generated events.

hydrodynamic models.^{10,13} The isotropic distribution of flow angles for small impact parameters is compatible with spherical-shaped distributions. A look at the shape parameters of the ellipsoids producing these flow angles verifies near-spherical shaped events. Thus at our level of statistics we do not find significantly oblate shapes in the Ar+Pb reaction. Indeed, recent hydrodynamical calculations for this reaction¹⁴ also show only slight deviations from spherical flow, at $b \rightarrow 0$. The cascade results presented in Fig. 2(b) exhibit considerable preference for the forward direction in both samples. This again reflects the lack of stopping power in this model.

The finite deflection angles observed for intermediate impact parameters in Fig. 2(a) make it possible to define a reaction plane by the incident beam direction and the direction of the major axis of the flux ellipsoid for each event. The reaction planes of all events can be aligned¹⁰ and the invariant cross section $d^3\sigma/dp_x dp_z dy$ analyzed as a function of rapidity y and transverse momentum components p_x and p_z , in plane and out of plane, respectively. This distribution projected onto the reaction plane is displayed in Fig. 3 for the intermediate impact parameter sample. A strong deflection away from the beam axis is observed further supporting the sideways preference of event flow angles observed in Fig. 2(a). Furthermore, when the events of Fig. 3 are projected perpendicular to the reaction plane, no sideways deflection appears and the results are

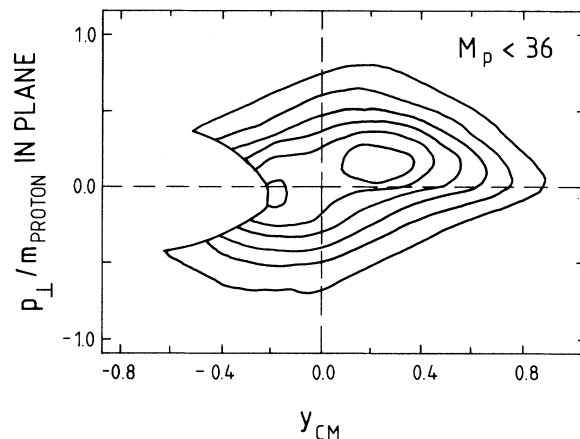


FIG. 3. Projection onto the reaction plane of the invariant proton cross section, shown by contour lines, for intermediate impact parameter Ar+Pb events which have been rotated into a common reaction plane orientation. The cutout at target rapidity reflects the target absorption losses.

symmetric with respect to the beam direction, lending further credence to the in-plane off-axis deflection. An analogous plot of the high multiplicity sample is consistent with spherical event shapes.

The sideways deflection has recently been observed for the high multiplicity near-central collisions of Nb+Nb.⁹ Such a deflection is observed in the present study of the asymmetric Ar+Pb system for intermediate impact parameters $3.0 \leq b \leq 5.5$ fm. A qualitative understanding of the difference in the impact parameter ranges can be found by considering the geometries of the two systems. In asymmetric systems such as Ar+Pb, collisions at small impact parameters result in the smaller projectile nucleus being completely engulfed by the heavy target nucleus. This is the case for the high multiplicity sample $b < 3$ fm for Ar+Pb where complete stopping is observed, the distributions finally become spherical, and no distinct sideways flow can develop. On the other hand, the intermediate impact parameter range for Ar+Pb corresponds to the Ar nucleus just reaching complete overlap with the Pb nucleus. This is analogous to small impact parameter collisions in a symmetric system such as Nb+Nb, thus accounting for the similarity of the observations.

In conclusion, collisions of ⁴⁰Ar with Pb at 0.772 GeV/u lead to a sideways deflection of the momentum flux at intermediate impact parameters in the vicinity of $b \sim 0.5b_{\max}$. This observation agrees qualitatively with the latest predictions of the hydrodynamical model^{13,14} providing evidence for the existence of a collective decompression in the flow of nuclear matter. For near-zero impact

parameters spherical momentum flow patterns are observed corresponding to complete stopping. The cascade model which neglects compressional degrees of freedom lacks this stopping power, suggesting the presence of a collective mechanism.

This work was supported in part by the U. S. Department of Energy under Contract No. DE-AC03-76SF00098.

¹M. I. Sobel, P. J. Siemens, J. P. Bondorf, and H. A. Bethe, Nucl. Phys. **A251**, 502 (1975).

²W. Scheid, H. Müller, and W. Greiner, Phys. Rev. Lett. **32**, 74 (1974); P. J. Siemens and J. O. Rasmussen, Phys. Rev. Lett. **42**, 844 (1979).

³J. Cugnon *et al.*, Nucl. Phys. **A352**, 505 (1981), and Phys. Rev. C **22**, 2094 (1981).

⁴J. Cugnon *et al.*, Phys. Lett. **109B**, 167 (1982).

⁵H. Stöcker *et al.*, Phys. Lett. **103B**, 269 (1981); J. I. Kapusta and D. Strottman, Phys. Rev. C **23**, 1282 (1981).

⁶M. Gyulassy *et al.*, Phys. Lett. **110B**, 185 (1982).

⁷J. Gosset *et al.*, Phys. Rev. C **16**, 629 (1977).

⁸R. Stock *et al.*, Phys. Rev. Lett. **44**, 1243 (1980).

⁹H. A. Gustafsson *et al.*, Phys. Rev. Lett. **52**, 1590 (1984).

¹⁰H. Stöcker *et al.*, Phys. Rev. C **25**, 1873 (1982); J. I. Kapusta and D. Strottman, Phys. Lett. **106B**, 33 (1981).

¹¹H. Ströbele *et al.*, Phys. Rev. C **27**, 1349 (1983).

¹²R. Stock *et al.*, Phys. Rev. Lett. **49**, 1236 (1982); J. W. Harris *et al.*, Lawrence Berkeley Laboratory Report No. LBL 17404 (to be published).

¹³H. Stöcker *et al.*, Phys. Rev. Lett. **52**, 1594 (1984).

¹⁴G. Graebner, thesis, University of Frankfurt, 1984 (unpublished).